Infrared absorption spectrum of B-doped Si

R. S. Leigh and M. J. L. Sangster
J. J. Thomson Physical Laboratory, University of Reading, Reading, Berkshire, England
(Received 19 July 1982)

It is shown that the presence of a sharp resonance (quasilocal mode) at 227 cm^{-1} in the one-phonon absorption spectrum associated with isolated boron substitutional impurities in silicon implies substantial stiffening of the bond-bending force constant at the impurity atom. Previous interpretations, in terms of the mass defect only, rely upon artificial assumptions concerning the host-lattice density of modes in the TA region. Changes in bond-bending and bond-stretching force constants are found by fitting to the quasilocal- and local-mode frequencies. Detailed calculations of the band absorption which include for the first time elements of the apparent charge tensor associated with first and second neighbors of the impurity (as well as the B^- impurity itself) are presented. These calculations illustrate the important effects of near-neighbor apparent charges on the strengths of the various features in the absorption spectrum. Asymptotic expressions are invoked to assign second-neighbor apparent-charge tensor elements, and the number of independent first-neighbor elements is reduced from three to two by application of a sum rule. The remaining two elements are fitted to the strengths of the 227-cm^{-1} quasilocal-mode absorption and the local-mode absorption. These apparent charges are then used in the calculations for the entire band. Parallels are drawn between the absorption peak around 330 cm^{-1} and the 227-cm^{-1} resonance. In an appendix it is shown that the contribution to the absorption arising from apparent charges on more distant neighbors (which are neglected in our calculations) is concentrated near the Raman frequency. In the band the integrated absorption from apparent charges on third neighbors and beyond is comparable with that from the apparent charges on the impurity and its first and second neighbors.

I. INTRODUCTION

The one-phonon absorption associated with substitutional boron in silicon has received considerable attention, both experimental and theoretical. A general discussion of the relevant experimental work and its interpretation is contained in the review by Newman.[1] For observation of the absorption associated with the impurity the crystal must be rendered transparent by removing free carriers through compensation. Compensation is achieved either by Li diffusion (e.g., Balkanski,[2] Spitzer and Waldner,[3] Chrenko *et al.*,[4] and more recently, Cardona, Shen, and Varma[5]), or by the inclusion of group-V dopants such as phosporus and the use of electron irradiation to obtain complete transparency (e.g., Angress, Goodwin, and Smith[6]). Only Angress *et al.*[6,7] and Cardona *et al.*[5] have measured the absorption over a wide range of frequencies in the host-crystal band; the measurements of other workers are confined to local modes and frequencies near the top of the band. The close proximity of an interstitial Li ion to a large proportion of the substitutional B impurities in the Li-compensated crystals complicates the interpretation of the absorption. Apart from some comments in Appendix C we shall therefore confine our attention to group-V—compensated crystals.

A feature of the band-mode absorption on which we shall concentrate attention is a sharp resonance (quasilocal mode) at 227 cm^{-1} which appears in both P- and As-compensated crystals[6,7] and is therefore presumed to arise from B. Any isotopic splitting that may be present is not resolved.

Neutron scattering studies of normal-mode frequencies in Si have been made by Dolling[8] at 296 K and by Nilsson and Nelin[9] at 300 K. These normal-mode frequencies are used in the next section to fit two parameters of the simple Keating[10] model which we adopt, namely nearest-neighbor bond-stretching and (essentially) bond-bending force constants. Our interest in the 227-cm^{-1} quasilocal mode was stimulated by observation of similar modes in GaAs (Ref. 11) and GaP.[12]

The local-mode frequencies and band-mode absorption were calculated by Dawber and Elliott[13] on the basis of a simple mass-defect model and a density of vibrational modes for Si due to Johnson (unpublished, but displayed by Dawber and Elliott).

Although this density of modes is considerably different from more recent calculations[14,15] based on more flexible models and fitted to dispersion data from the neutron scattering studies, the main transverse-optical (TO) peak is at approximately the right frequency. The overestimates of the local-mode frequencies by Dawber and Elliott indicate that changes in the force constants around the B impurities have to be considered. The Johnson density of modes falls to a very low minimum at around 150 cm^{-1} compared with around 225 cm^{-1} in the Weber[15] model. Dawber and Elliott find evidence of a quasilocal mode for B in Si just above this frequency (i.e., 150 cm^{-1}). It is tempting to consider that a suitable correction of the density of modes would lead to an accurate prediction of the 227-cm^{-1} resonance from simple mass-defect theory without any changes in force constant. Cardona *et al.*[5] have made such a calculation, but for this purpose they replace the density of transverse-acoustic (TA) modes by a rectangle extending from 100 to 215 cm^{-1}. The artificially introduced abrupt fall in the density of modes at the top of the TA region (which is also an incorrect feature of Johnson's distribution) leads inevitably to a quasilocal mode for any impurity mass lighter than the host mass. In fact, Cardona *et al.* find it to be only 0.8 cm^{-1} above 215 cm^{-1}. Our dynamical model agrees with Weber's in showing a considerably less abrupt fall in the density of modes. We have carried out a mass-defect calculation (with no changes in force constants) using our dynamical model and making the usual assumption that only the motion of the impurity contributes to the dipole moment. As discussed by Leigh and Szigeti[16] this assumption is incorrect but corresponds to that made by Cardona *et al.* (and by Dawber and Elliott). We find a broad peak just above the peak in the density of modes, in complete agreement with the result of Cardona *et al.* using Weber's density of modes (actually for Ge with an appropriate change in frequency scale). We feel that it is misleading to describe this resonance as a quasilocal mode when it occurs at a frequency (219 cm^{-1}) at which the density of modes is still $\sim 70\%$ of its value at the 215-cm^{-1} peak and the resonance is correspondingly broad.

We also find, as in the work of Dawber and Elliott, that the local-mode frequencies are too high. In Sec. III it will be shown that around the B impurity, in addition to a reduction in the B-Si bond-stretching force constant to lower the local-mode frequencies, a stiffening of the Si-B-Si bond-bending force constant is required to produce the quasilocal mode. A similar conclusion was reached by Talwar and Agrawal[17] in their explanation of the low-frequency part of the infrared absorption of Be-doped ZnS, although the resonance in this system (at 132 cm^{-1}, Ikuta *et al.*[18]) which parallels the feature under discussion here is explained, at least approximately, without a bond-angle force-constant change. While the work of Talwar and Agrawal is in some of its aspects similar in spirit to that presented here, their assumption that only the apparent charge on the impurity need be considered seems to us to invalidate much of their discussion of the relative intensities of features in the absorption spectrum.

The calculations presented here have two main aims. First, we show that with a reasonably good (albeit simple) model for the dynamics of the perfect lattice the local-mode and quasilocal-mode frequencies can be explained by force-constant changes which, as will be argued in Sec. III, are physically plausible. Second, we demonstrate in Sec. V that in order to understand the intensities of features in the band absorption it is essential to take into account apparent charges on host atoms as well as the impurity. It was shown by Leigh and Szigeti[16,19–21] that the existence of these additional apparent charges follows inescapably from macroscopic considerations. We believe that the present calculations are the first to examine this effect in detail. A preliminary account of this work has recently appeared.[22]

II. LATTICE DYNAMICAL MODEL

For the dynamics of the Si lattice we use the simple Keating[10] model which has only two parameters, a nearest-neighbor bond-stretching force constant α, and a bond-angle force constant β. The corresponding energy changes are

$$\tfrac{1}{2}\alpha\left[\frac{3}{4r_0^2}\right][\delta(r^2)]^2$$

per bond and

$$\tfrac{1}{2}\beta\left[\frac{3}{4r_0^2}\right][\delta(\vec{r}_1\cdot\vec{r}_2)]^2$$

per bond pair, where r_0 is the equilibrium nearest-neighbor distance ($r_0=\sqrt{3}a/4$ with a the side of the elementary face-centered cube). Although more sophisticated models are available, such as the bond-charge model of Weber[15] which agrees well with all measured phonon frequencies, the relevant characteristics of the density of modes may be adequately represented by the simpler two-parameter model.

The simplicity of the model has the consequence that no particular choice of the two parameters will reproduce all measured frequencies. Different choices may be appropriate to different applications. Thus Martin[23] gives one choice which reproduces

the three elastic constants to within 1%, and Baraff *et al.*[24] give a rather different choice which is constrained to fit the compressibility and reproduce phonon frequencies in the part of the zone particularly relevant to the vacancy problem which they consider. In our case we have two essential requirements: To treat the local modes we need a good representation of the highest-frequency peak in the density of modes and for the quasilocal mode we need, as has been discussed in the Introduction, a faithful reproduction of the falloff to the low minimum at 227 cm^{-1}. The first requirement is met by fitting to the frequency of the TO phonon at the L point (L_3') which Dolling[8] gives as 14.68±0.30 THz. Comparison of the dispersion curves with the density of modes suggests a correlation between the low minimum in the density and the maximum in the $\Sigma_3(A)$ branch, which the interpolated measurements of Nilsson and Nelin[9] show to be at a wave vector of (0.67, 0.67, 0)π/a with a frequency of 6.80 (±0.06) THz. We have forced the maximum in the $\Sigma_3(A)$ branch of the model to equal 6.80 THz, and it then occurs at (0.69, 0.69, 0)π/a. It is, of course, possible that the edge to the low minimum arises from phonons in lower symmetry directions, but our subsequent calculation of the density of modes rules this out for the Keating model at least.

In Table I we list our force constants for silicon together with those for the other applications of the Keating model mentioned above. The density of modes from our choice of parameters is shown in Fig. 1 with the results of Weber for comparison. (We take the Weber calculation to be the best available interpolation of the existing measurements along high-symmetry directions.) In addition to the two fitted frequencies there is excellent agreement in the edge to the low minimum (227 cm^{-1}) and in the features at 215 cm^{-1} and around 325 cm^{-1}, and fairly good agreement around 400 cm^{-1}. The Keating model fails to give the characteristic flattening of the TA branch and hence the associated sharp peak in the spectrum. Also the splitting of the TO peak and its tail to the Raman frequency are not reproduced. These shortcomings are unlikely to prove serious in our application.

TABLE I. Force constants (in $N\,m^{-1}$) for Keating model for Si.

	α	β
This work	46.05	7.10
Martin[a]	48.50	13.81
Baraff *et al.*[b]	51.51	4.70

[a]Reference 23.
[b]Reference 24.

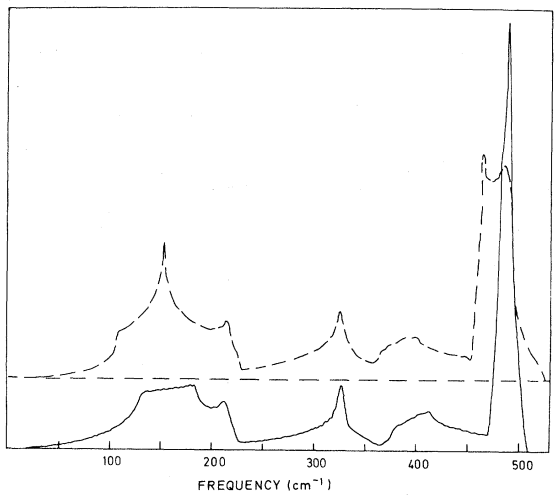

FIG. 1. Density of modes for Si. Solid curve is for the Keating model with $\alpha=46.05$ N/m and $\beta=7.10$ N/m; dashed curve is from Weber (Ref. 15).

III. FORCE CONSTANT CHANGES AROUND THE IMPURITY

The cross section for infrared absorption induced by a defect at a site of cubic symmetry in a crystal of refractive index ρ [3.414 at 296 K (Ref. 25)] can be written as

$$\sigma(\omega)=\frac{4\pi\omega}{\rho c}\sum_{n\alpha}\sum_{n'\beta}\eta^z_{n\alpha}\eta^z_{n'\beta}\mathrm{Im}G'_{n\alpha;n'\beta}(\omega)\ , \qquad (3.1)$$

where the summations are over atomic sites and Cartesian components of displacement. The functions $G'_{n\alpha;n'\beta}(\omega)$ are the (Cartesian) Green's functions for the lattice containing the defect and the coefficients $\eta^z_{n\alpha}$ are the apparent charges (in the terminology of Leigh and Szigeti[16])

$$\eta^z_{n\alpha}=\frac{\partial M_z}{\partial u_{n\alpha}} \qquad (3.2)$$

with M_z the z component of the total dipole moment and $u_{n\alpha}$ the α component of the displacement of the nth atom. The derivative is to be taken at constant macroscopic electric field; this is equivalent to the use of slab geometry in Ref. 16. Equation (3.1) follows from Eq. (1.15) of Maradudin[26] with some changes in notation and a simplification for the cubic symmetry of the defect site. Equation (3.1) can be written in a contracted matrix notation as

$$\sigma(\omega)=\frac{4\pi\omega}{\rho c}\tilde{\underline{\eta}}\,\underline{\underline{G}}'(\omega)\underline{\eta} \qquad (3.3)$$

with $\underline{\eta}$ the vector of apparent charges and transposition denoted by a tilde. Since only displacements of

Γ_5 symmetry are infrared active, reduction in the number of terms to be considered results from projecting out these symmetry-adapted displacements. Writing the vector of symmetry-adapted displacements transforming as row z of the Γ_5 irreducible representation as $\underline{d}(\Gamma_5)$ and the vector of atomic Cartesian displacements as $\underline{u}$ (corresponding to $\underline{\eta}$) we have the transformations

$$\underline{u}=\underline{\underline{S}}\,\underline{d}(\Gamma_5),\quad \underline{d}(\Gamma_5)=\underline{\underline{\tilde{S}}}\,\underline{u} \tag{3.4}$$

and hence

$$\sigma(\omega)=\frac{4\pi\omega}{\rho c}\underline{\tilde{\eta}}(\Gamma_5)\underline{\underline{G}}'(\Gamma_5{:}\omega)\underline{\eta}(\Gamma_5) \tag{3.5}$$

with

$$\underline{\underline{G}}'(\Gamma_5{:}\omega)=\underline{\underline{\tilde{S}}}\,\underline{\underline{G}}'(\omega)\underline{\underline{S}} \tag{3.6}$$

and

$$\underline{\eta}(\Gamma_5)=\underline{\underline{\tilde{S}}}\,\underline{\eta}\ . \tag{3.7}$$

We shall consider apparent charges on the impurity atom, its four first (111-type) neighbors and its twelve second (220-type) neighbors. With this restriction $\underline{\eta}$ (or $\underline{u}$) is a 51-component vector. There are eight occurrences of Γ_5 in this subspace: one for the impurity itself, two for the first neighbors, and five for the second neighbors. The transformation matrix $\underline{\underline{S}}$ is then 51×8. The elements of $\underline{\underline{S}}$ are obtained by standard group-theoretical arguments and depend on the choice made for the symmetry-adapted displacements. Our choice is shown in Fig. 2.

The 8×8 (symmetric) Green's function matrix for the defect lattice, $\underline{\underline{G}}'(\Gamma_5{:}\omega)$, is obtained in the usual way, e.g., Maradudin,[26] from its counterpart for the perfect lattice $\underline{\underline{G}}(\Gamma_5{:}\omega)$:

$$\underline{\underline{G}}'(\Gamma_5{:}\omega)=[\underline{\underline{I}}+\underline{\underline{G}}(\Gamma_5{:}\omega)\underline{\underline{D}}(\Gamma_5{:}\omega)]^{-1}\underline{\underline{G}}(\Gamma_5{:}\omega) \tag{3.8}$$

with $\underline{\underline{D}}(\Gamma_5{:}\omega)$ the symmetry-reduced defect matrix which, with our assumptions, is nonzero only in the subspace containing the impurity and its nearest neighbors [leading to the usual simplifications in the matrix inversion in Eq. (3.8)]. The nonzero part of $\underline{\underline{D}}(\Gamma_5{:}\omega)$ is given in terms of the force-constant changes $\delta\alpha$ (for B—Si bonds) and $\delta\beta$ (for Si—B—Si bond pairs) and the mass defect $\delta m=m_{\mathrm{B}}-m_{\mathrm{Si}}$:

$$\begin{bmatrix} 4\delta\alpha+2\delta\beta-\delta m\omega^2 & -2\sqrt{2}\delta\alpha+\sqrt{2}\delta\beta & -2\delta\alpha-\delta\beta \\ -2\sqrt{2}\delta\alpha+\sqrt{2}\delta\beta & 2\delta\alpha+\delta\beta & \sqrt{2}\delta\alpha-\frac{1}{2}\sqrt{2}\delta\beta \\ -2\delta\alpha-\delta\beta & \sqrt{2}\delta\alpha-\frac{1}{2}\sqrt{2}\delta\beta & \delta\alpha+\frac{1}{2}\delta\beta \end{bmatrix}, \tag{3.9}$$

where the row and column ordering corresponds to that of the (first three) displacements in Fig. 2.

$\underline{\underline{G}}(\Gamma_5{:}\omega)$, being 8×8 and symmetric, is specified by 36 functions of frequency which can be obtained from a smaller number of independent $G_{n\alpha;n'\beta}(\omega)$. The eight classes of atom pairs which have to be considered are identified in Table II by their typical separation vectors (in units of $a/4$). Also listed are the numbers of independent Green's-function components for the eight classes. It may be noted that the symmetry of the Green's functions is the same as that of force constants required to specify general interactions between pairs of atoms. Herman[27] details the symmetry transformations relating force-constant matrices for different members of a class. It can be seen from Table II that 26 perfect-lattice functions $G_{n\alpha;n'\beta}(\omega)$ are required.

The procedure then consists of the following steps:

(a) calculate the 26 independent perfect lattice functions,

(b) set up the full 51×51 matrix $\underline{\underline{G}}(\omega)$ and project out the symmetrized matrix $\underline{\underline{G}}(\Gamma_5{:}\omega)$ as in Eq. (3.6), and

(c) calculate the modified matrix for the defect crystal using Eq. (3.8).

If the apparent charges are known, the absorption

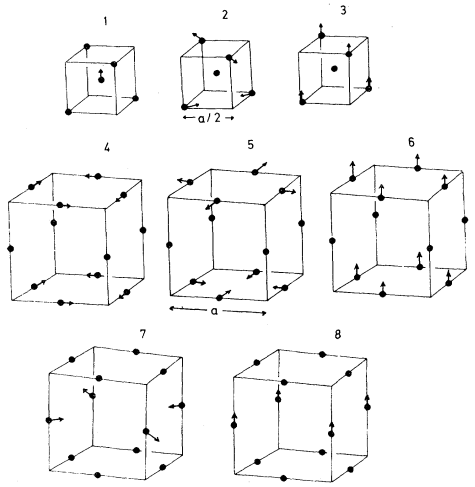

FIG. 2. Symmetry-adapted displacements for row z (vertically upwards in the figure) of the Γ_5 representation. Number 1 refers to the impurity, 2 and 3 to its first neighbors and 4—8 to its second neighbors.

TABLE II. Classes of atom pairs in a complex consisting of an atom and its first and second neighbors.

Class	Pair separation vector (units of $a/4$)			Number of independent Green's functions
1	0	0	0	1
2 (1st NN)	1	1	1	2
3 (2nd NN)	2	2	0	4
4 (3rd NN)	−3	−1	−1	4
5 (4th NN)	4	0	0	2
6 (5th NN)	3	3	1	4
7 (6th NN)	4	2	2	5
8 (9th NN)	4	4	0	4

cross section is given by Eq. (3.5). The above steps can be seen to follow the procedure of Talwar and Agrawal[28] with extensions to include apparent charges on the first and second neighbors of the impurity.

The 26 perfect-lattice Green's functions $G_{n\alpha;n'\beta}(\omega)$ are calculated from the eigenvectors at a sample of $\vec{q}$ vectors by fairly standard methods which will be outlined only briefly. The eigenvectors and frequencies are calculated at 6336 regularly spaced points in the symmetry-reduced zone (1/48th) corresponding to 64^3 points in the full zone. The contributions at a particular eigenfrequency to the imaginary parts of the Green's functions are obtained from the corresponding eigenvectors taking due account of phase differences between cells and the summation over the components of the star of the $\vec{q}$ vector. The imaginary parts are histogrammed in frequency with a bin width of 1 cm^{-1}, and then each histogram rectangle is replaced by a truncated quartic function of the same area centered on the middle of the division and set to zero with zero slope at ± 3 cm^{-1} from the center. In addition to providing smoother functions, this last step allows analytic evaluation of the principal-value integrals required for obtaining the real parts of the Green's function by Hilbert transformation. (This unpublished method was introduced to us by J. Slater.)

Step (c) requires values for the force-constant changes $\delta\alpha$ and $\delta\beta$. The mass defect δm is of course known. We obtain values by fitting to the observed local-mode and quasilocal-mode frequencies for the ^{11}B impurity. Outside the band ($\omega > \omega_R$) $\underline{\underline{G}}$ is real. The local-mode frequency is therefore fitted exactly if the force-constant changes are chosen so that the determinant

$$|\underline{\underline{I}} + \underline{\underline{G}}(\Gamma_5{:}\omega)\underline{\underline{D}}(\Gamma_5{:}\omega)|$$

is zero at that frequency [cf. Eq. (3.8)]. In the band ($\omega < \omega_R$) $\underline{\underline{G}}$ is complex, but in the neighborhood of the resonance frequency the imaginary parts of its elements are small due to the low minimum in the density of modes. We may therefore fit the resonance frequency approximately be neglecting the imaginary parts altogether and proceeding as for the local mode. In subsequent calculations of the absorption spectrum [taking proper account of the imaginary parts (cf. Sec. V)] we find that the frequency of the maximum of the resonance peak is ~ 1 cm^{-1} higher than the frequency as fitted above. (A shift upwards is to be expected when imaginary parts are decreasing.) We therefore choose the force-constant changes to make the determinant vanish at 226 cm^{-1}. (Identifying the frequency of the undamped resonance with the vanishing of the above determinant is only one of several alternative procedures. This is discussed in Appendix A where we show that at least in the present case the alternative identifications agree to within ~ 0.1 cm^{-1} for a given choice of force-constant changes.)

As suggested by Angress *et al.*[11] the local-mode frequency is relatively insensitive to changes in the bond-bending force constant ($\delta\beta$) but the frequency of the resonance depends more strongly on $\delta\beta$ than on $\delta\alpha$. Fitting the frequencies of the ^{11}B local mode[6] (620.2 cm^{-1}) and the resonance requires the following force-constant changes (in $N\,m^{-1}$):

$$\delta\alpha = -6.34, \quad \delta\beta = 7.55 , \tag{3.10}$$

i.e., the bond-stetching force constant around the B impurity is 0.86 of that in the host crystal, and the corresponding ratio for bond bending is 2.1. With these force-constant changes the ^{10}B local-mode frequency is 644.4 cm^{-1}, in satisfactory agreement with the experimental value of 643.9 cm^{-1} (Angress *et al.*[6]). The frequency of the quasilocal mode (227 cm^{-1}) is practically independent (~ 0.2 cm^{-1}) of which B isotope is substituted. Many atoms participate in the quasilocal mode, and the displacement of the impurity itself is comparable with those of the surrounding host atoms.

While the modest reduction in the force constant α around the impurity is of reasonable magnitude and the expected sign (since the boron atom is smaller than the silicon atom which it replaces), the enhancement of the bond-bending force constant by a factor of 2.1 requires some discussion. Angress *et al.*[11] have already pointed out from the tabulations by Herzberg[29] that the bend to stretch ratio in XY_4 molecules is markedly higher for a given Y with X=C than with X=Si. The force-constant ratios around B and C are likely to be similar since both are second-row elements. The same conclusion follows from a comparison of the Keating force constants in diamond and Si. Martin[23] finds β/α ratios of 0.655 in diamond and 0.285 in Si. Our ra-

tio in Si is 0.154 (since we adopt a lower value for β) and around a B impurity 0.369. Thus it can be seen that our large enhancement of β is roughly consistent with the β/α ratio depending predominantly on the row of the Periodic Table from which the atom comes.

IV. APPARENT CHARGES

A. Apparent charges on second neighbors

Macroscopic arguments[16,21] lead to the following expressions which are asymptotically exact at large distances from a charged impurity in the diamond structure:

$$\eta^z_{nx}=\frac{Ze\epsilon_0}{32\pi}\left[\frac{a}{r}\right]^3\left[-(p_{12}+p^0_{44})\frac{3xz}{r^2}\pm 2\beta_R y\right],$$

$$\eta^z_{ny}=\frac{Ze\epsilon_0}{32\pi}\left[\frac{a}{r}\right]^3\left[-(p_{12}+p^0_{44})\frac{3yz}{r^2}\pm 2\beta_R x\right], \tag{4.1}$$

$$\eta^z_{nz}=\frac{Ze\epsilon_0}{32\pi}\left[\frac{a}{r}\right]^3(p_{11}-p^0_{44})\left[1-\frac{3z^2}{r^2}\right].$$

Here Ze denotes the net static charge associated with the impurity ($Z=-1$ for B in Si), ϵ_0 ($=\rho^2$) denotes the static dielectric constant of the host crystal, and $\vec{r}$ (with components x,y,z) is the position vector of the nth atom relative to the impurity. The p coefficients are the conventional photoelastic constants, except that p^0_{44} denotes the value that p_{44} would have if the relative displacement of the two sublattices in the z direction were fixed during the xy shear. The quantity β_R is proportional to the only nonvanishing element of the Raman tensor, i.e.,

$$\epsilon_0^2\beta_R=\frac{\partial\epsilon_{xy}}{\partial u_z}=\frac{\partial\epsilon_{yz}}{\partial u_x}=\frac{\partial\epsilon_{zx}}{\partial u_y},$$

where ϵ_{xy}, etc., are elements of the static dielectric tensor and $\vec{u}$ denotes the relative sublattice displacement. If $\vec{u}$ is defined as the displacement of the A sublattice relative to that of the B sublattice then the upper or lower sign in front of the β_R terms in (4.1) applies according as the nth atom is on the A or B sublattice. The β_R terms represent the apparent charges induced by the electric field itself while the photoelastic terms represent the apparent charges induced by its gradient. The physics of the β_R terms is the same as that of the first-order infrared absorption observed in pure diamond-structure crystals in the presence of a *uniform* electric field.[30,31] The relationship between p^0_{44} and the observed p_{44} is given by

$$p_{44}=p^0_{44}-(1/\sqrt{3})\beta_R r_0\zeta, \tag{4.2}$$

where ζ is the dimensionless quantity introduced by Kleinman[32] to describe the sublattice displacement accompanying shear, i.e.,

$$\frac{1}{\sqrt{3}}r_0\zeta=\frac{\partial u_z}{\partial S_{xy}}=\frac{\partial u_x}{\partial S_{yz}}=\frac{\partial u_y}{\partial S_{zx}},$$

where S_{xy}, etc., are elements of the strain tensor.

We assume (cf. the discussion by Leigh and Szigeti[20]) that expressions (4.1) apply to all atoms beyond nearest neighbors of the impurity. This assumption is not unreasonable (as it would be for nearest neighbors), and it serves to keep to a minimum the number of apparent charges to be inferred from analysis of the observed impurity absorption. In our calculations of the spectral dependence of the absorption cross section we neglect apparent charges on third neighbors and beyond so that expressions (4.1) are used in these calculations only for second neighbors. We can, however, calculate the total *integrated* one-phonon absorption arising from third neighbors and beyond according to (4.1) by using the result [see, for example, Leigh and Szigeti[16] or Maradudin,[26] Eq. (1.16a)]

$$\int\sigma(\omega)d\omega=\frac{2\pi^2}{\rho c}\left[\frac{\eta_0^2}{m_{\mathrm{B}}}+\frac{1}{m_{\mathrm{Si}}}\sum_n{}'[(\eta^z_{nx})^2+(\eta^z_{ny})^2+(\eta^z_{nz})^2]\right], \tag{4.3}$$

where the prime on the summation means that the sum extends over all host atoms.

In Appendix B we discuss the available experimental values for the photoelastic constants and the Raman constant. We adopt the following values:

$$p_{11}=-0.093,$$

$$p_{12}=+0.019,$$

$$p_{44}=-0.050,$$

and

$$\beta_R r_0=-0.1.$$

The resulting values of the second neighbor apparent charges are given in Table III.

B. Apparent charges on first neighbors

Macroscopic arguments[19,21] show that

TABLE III. Apparent charges (in units of $|e|$) on second neighbors of the impurity, calculated from (4.1) with $Z=-1$, for the impurity on a site with a nearest neighbor at $\frac{1}{4}a(1,1,1)$. Only symmetrically inequivalent apparent charge elements are given.

Site of atom n	α	$\eta^z_{n\alpha}$
$\frac{1}{4}a(0,2,2)$	x	+0.076
	y	−0.033
	z	−0.001
$\frac{1}{4}a(2,2,0)$	x	+0.076
	z	+0.002

$$\eta_0+\sum_n{}' \eta^z_{nz}=SZe\ , \tag{4.4}$$

where

$$S=1+\tfrac{1}{3}\epsilon_0(p_{11}+2p^0_{44})\ . \tag{4.5}$$

With the values adopted in the preceding section we find $S=-0.03$. To the level of accuracy represented by the uncertainties in p_{11}, p_{44}, and β_R this means that S is zero.

The summation on the left-hand side of (4.4) extends over all host atoms. It converges more rapidly than might be expected because in tetrahedral symmetry the sum over a single shell of atoms becomes zero when the η^z_{nz} are given by the asymptotic expressions (4.1).[19] The assumption made in the preceding section that the apparent charges of all atoms beyond first neighbors of the impurity are given by (4.1) therefore implies that only first neighbors contribute to the summation.

By symmetry η^z_{nz} is the same for all four nearest neighbors, and so is equal to $-\frac{1}{4}\eta_0$. We denote it by $\eta_1^{\parallel}$. The off-diagonal apparent charges of the first neighbors are all the same except for sign. For a (111) neighbor they are equal and we denote them by $+\eta_1^{\perp}$.

C. Adjustment to experiment

We are left with two adjustable apparent charges, η_0 and $\eta_1^{\perp}$. We choose these to make the integrated absorption of the ^{11}B local mode and 227-cm^{-1} quasilocal mode agree with experiment. Since the absorption is quadratic in the apparent charges there are four alternative sets of values of η_0 and $\eta_1^{\perp}$. In the next section we shall compare with experiment the absorption over the entire band region; this is different for the four sets.

For the local mode we use the room-temperature result of Goodwin,[33] viz., 0.059 eV cm^{-1} for a total boron concentration of 5×10^{19} cm^{-3}. Assuming the natural isotopic abundance, the integrated cross section of ^{11}B (frequency in cm^{-1}) is 117×10^{-19} cm. Fitting the strength of the quasilocal mode requires care for several reasons:

(a) the theoretical width turns out to be not much more than half that observed;

(b) it is not known how much of the experimental "background" arises from processes other than one-phonon absorption (e.g., the low-frequency tail of the interband absorption, or residual free-carrier absorption);

(c) although both experimentally and theoretically the absorption on the high-frequency side of the resonance is less than that on the low-frequency side, the asymmetry of the calculated line shapes is different for the four sets of apparent charges.

However, we find that for all four sets of apparent charges the following procedure leads to agreement between the observed and calculated integrated cross sections to within $\sim10\%$ whatever truncations are used. We treat the resonance as if it were a true local mode, i.e., we neglect the imaginary part of the Green's functions, (see Appendix A) and fit to a value of 2.6×10^{-19} cm for the strength of the δ function in the cross section for ^{11}B. It is important to note that this is *not* equal to any reasonable estimate of the observed area of the peak above background: it is in fact more than double. In other words, when the imaginary parts are included the excess goes into the background.

We give in Table IV the four sets of values of η_0, $\eta_1^{\parallel}$, and $\eta_1^{\perp}$. We recall that the apparent charges on second neighbors are the same in all four sets (and are given in Table III). The four sets are characterized by the signs (relative to the B displacement) of (a) the dipole moment of the local mode and (b) the dipole moment which is associated with the quasilocal mode when the imaginary parts of the Green's functions are neglected. These dipole moments are sums of the products of apparent charges and the corresponding displacements, the latter being given by the mode eigenvectors. In Table V we show the contributions to these sums from η_0, $\eta_1^{\parallel}$, $\eta_1^{\perp}$, and second neighbors. The dipole moment of the local

TABLE IV. Alternative sets of apparent charges (in units of $|e|$) on the impurity and its first neighbors.

	A	B	C	D
η_0	−0.938	−0.821	+0.827	+0.944
$\eta_1^{\parallel}$ $(=-\frac{1}{4}\eta_0)$	+0.235	+0.205	−0.207	−0.236
$\eta_1^{\perp}$	+0.013	+0.261	−0.272	−0.025

TABLE V. Contributions to mode dipole moments $\partial M/\partial Q$ (in units of $|e|/\sqrt{m_{Si}}$) from apparent charges on the impurity (^{11}B) and its first and second neighbors for the alternative sets of apparent charges. (Q is a normal mode coordinate.) The upper of each pair of numbers refers to the local mode, the lower to the quasilocal mode at 227 cm^{-1}.

	A	B	C	D
η_0	−1.336	−1.170	+1.178	+1.345
	−0.335	−0.293	+0.295	+0.337
$\eta_1^{\parallel}$	−0.165	−0.144	+0.145	+0.166
	+0.077	+0.068	−0.068	−0.078
$\eta_1^{\perp}$	−0.010	−0.197	+0.205	+0.019
	+0.022	+0.444	−0.463	−0.043
2nd NN	−0.009	−0.009	−0.009	−0.009
	+0.009	+0.009	+0.009	+0.009

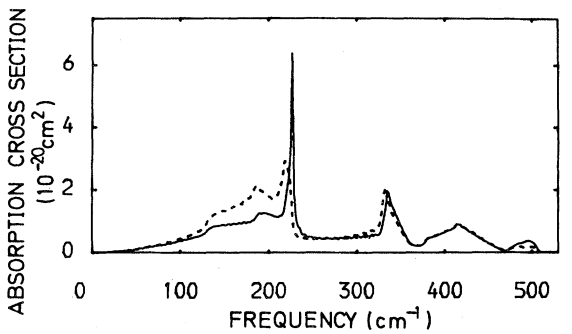

FIG. 3. Absorption cross section for substitutional ^{11}B in Si on the assumption that only the impurity carries an apparent charge (η_0). Solid curve is for $\delta\alpha=-6.34$ N/m, $\delta\beta=7.55$ N/m, and $\eta_0=\pm1.067|e|$; dotted curve is for $\delta\alpha=-4.13$ N/m, $\delta\beta=0$, and $\eta_0\pm1.084|e|$.

mode is dominated by the contribution of η_0 and so is negative for sets A and B and positive for sets C and D. The dipole moment of the quasilocal mode is negative in sets A and C and positive in sets B and D.

We note that if η_0 and $\eta_1^{\perp}$ are given values which are the arithmetic means of sets A and B on the one hand, or of sets C and D on the other, the quasilocal mode does not absorb at all. Within the present context the actual values of η_0 and $\eta_1^{\perp}$ in each of the four sets are therefore determined rather well by the strength of the quasilocal mode.

V. BAND ABSORPTION SPECTRUM

In this section we discuss the entire band spectrum. Results are given for ^{11}B, but there is no significant change in going to ^{10}B. We first present, in Fig. 3, band-absorption spectra calculated on the assumption that only the impurity atom carries an apparent charge (η_0). Although this assumption is certainly false it serves to separate the effects of increasing the Si-B-Si angle force constant from the effects of including apparent charges on neighbors of the impurity. The dotted curve in Fig. 3 shows the absorption cross section calculated without any change in the bond-angle forces ($\delta\beta=0$) but with a decrease in the B-Si stretch constant from the pure Si value ($\delta\alpha=-4.13$ N m^{-1}) chosen to bring the ^{11}B local-mode frequency into agreement with experiment. η_0 ($=\pm1.084|e|$) is chosen to give the observed local-mode strength. There is a peak in the cross section at 219 cm^{-1}, but this is significantly lower than 227 cm^{-1} and in fact only 4 cm^{-1} higher than the peak in the density of modes. There is also a second peak of similar strength at 187 cm^{-1}, but this is associated with the X_3(TA) critical point which is placed at 185 cm^{-1} by our Keating model instead of the observed 150 cm^{-1}. A simple mass-defect calculation ($\delta\alpha=\delta\beta=0$) gives a spectrum which is virtually indistinguishable in the band from the dashed curve but has the ^{11}B local mode at 645.8 cm^{-1}.

The solid curve in Fig. 3 shows the cross section calculated with the force-constant changes (3.10), i.e., with $\delta\alpha$ and $\delta\beta$ fitted to the observed ^{11}B local-mode frequency and the 227-cm^{-1} peak, but still with an apparent charge only on the impurity and chosen ($\eta_0=\pm1.067|e|$) to give the observed local-mode strength. Although there is now a peak at 227 cm^{-1} (because fitted) its strength above the background is about 3 times that of the observed peak. Also the absorption feature around 330 cm^{-1} is more prominent than that around 420 cm^{-1}, and there is very little absorption just below the Raman frequency, in marked disagreement in both cases with the observed spectrum.

The solid curves in Fig. 4 show the band spectra calculated with the four sets of apparent charges of Table IV in conjunction with the force-constant changes (3.10). The dashed curves show the spectra calculated with the second-neighbor apparent charges omitted but those of the impurity and its first neighbors as in Table IV. It will be seen that with sets A and C the main effect of the second neighbors is to produce a large increase of absorption in the optical region, though there is also some redistribution at lower frequencies. With sets B and D, on the other hand, the main effect is an increase in the acoustic region of the spectrum. With set B this is actually accompanied by a decrease in the optical region. In Table VI the integrated cross section is broken down in two ways for each of the four sets of apparent charges: first into the contributions from the local mode (fitted) and from the band, then into the contributions from the impurity and its first

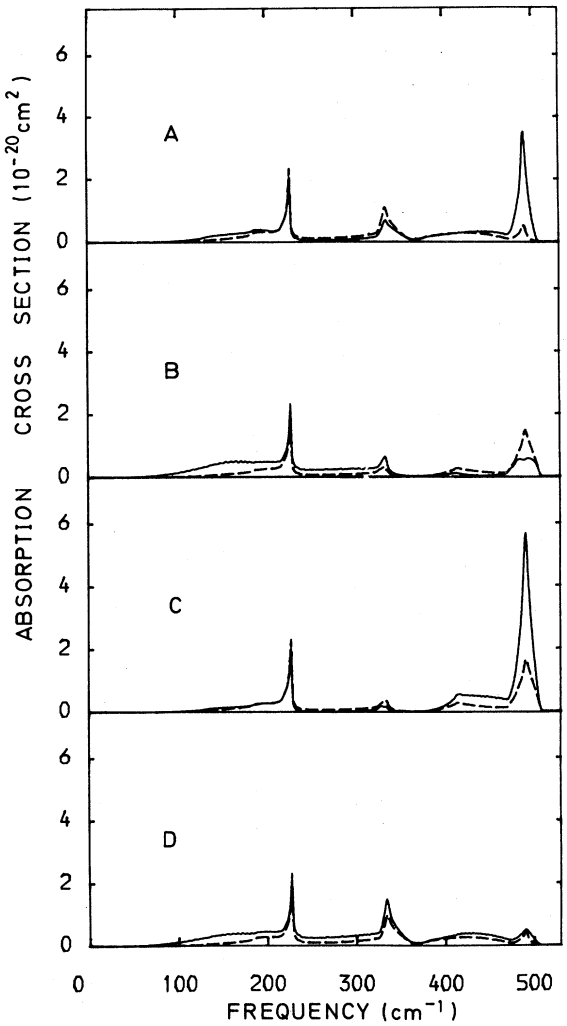

FIG. 4. Absorption cross section for substitutional ^{11}B in Si with apparent charges on the impurity and its first and second neighbors. Solid curves are for the four alternative sets of apparent charges given in Table IV (impurity and first neighbors) together with those of Table III (second neighbors). Dashed curves are for the apparent charge sets of Table IV with second-neighbor apparent charges neglected.

and second neighbors as given by terms of the sum in Eq. (4.3).

The complete absence of absorption by long-wave acoustic modes for all four sets of apparent charges (see Fig. 4 and compare with Fig. 3) follows from the zero value of S in Eq. (4.4), since in these modes each B impurity is moving rigidly with its Si neighbors. This is in contrast to the situation in the optical part of the spectrum, and the local mode, where the Si neighbors move against the B impurity and so increase the dipole moment (cf. Table V).

The total contribution to the integrated cross section from third neighbors and beyond may be calculated from Eq. (4.3) using the asymptotic values of the apparent charges given by Eqs. (4.1). We have carried out summations for the first few shells exactly, the remainder being estimated by an integral. We find 0.24 in the units of Table VI (12×10^{-19} cm). Since the photoelastic parts of the apparent charges fall off as the field gradient and the Raman parts as the field, the latter predominate, and in Appendix C we show that their contribution to the absorption is expected to appear just below the Raman frequency. It will be noted that the contribution to the integrated cross section from third neighbors and beyond is as large as the *entire* band absorption provided by the impurity and its first and second neighbors. Moreover, since the effect depends only on the presence of a charged center, there is an equal contribution from the compensating impurity. Therefore only *half* the observed absorption should be compared with 0.24. Referring to the boron-arsenic spectrum of Angress *et al.*,[7] the *total* integrated one-phonon absorption between the minimum around 450 cm^{-1} (56 meV) and the Raman frequency is, with a reasonable assumption about the sloping background, ~0.3 (again in the units of Table VI). This suggests that our choice of 0.1 for $|\beta_R r_0|$ is too high (its *square* by a factor of between 2 and 3 depending on which set of apparent charges is taken). We note that although the wide range of possible values for $|\beta_R r_0|$ (see Appendix B) does extend below 0.1, it also extends to more than twice this. It is of course possible that the impurity concentration in the sample has been overestimated. Alternatively the theoretically predicted cross section may be too large because of the effects of correlations between the positions of impurity atoms. This is discussed in Appendix C.

Is it possible to choose between the four sets by a detailed comparison of the calculated and observed spectra? It must be recalled that[1] a feature common to the observed spectra of crystals doped with

TABLE VI. Integrated absorption cross section broken down in two ways for the alternative sets of apparent charges. If frequency is in cm^{-1} the units are $\pi e^2/(\rho c^2 m_{Si})=5.065\times10^{-18}$ cm. Apparent charges on third and further neighbors of the impurity are neglected.

	A	*B*	*C*	*D*
Local mode	2.31	2.31	2.31	2.31
Band	0.26	0.23	0.30	0.29
Impurity (^{11}B)	2.25	1.72	1.75	2.28
1st NN	0.22	0.71	0.76	0.23
2nd NN	0.10	0.10	0.10	0.10

boron-phosphorus and boron-arsenic could be due to

(i) isolated substitutional boron atoms,

(ii) isolated interstitial boron atoms,

(iii) boron pairs, or

(iv) defects (e.g., divacancies) produced by the electron irradiation used to render the specimens transparent.

For all four sets of apparent charges there is an absorption feature around 330 cm^{-1} (41 meV) associated with a strong peak in the density of modes. The experimental spectra[7] for boron-phosphorus and boron-arsenic both show a feature at this frequency which to judge from a comparison of the two spectra is very minor, certainly much weaker than the 227-cm^{-1} resonance. This seems sufficient reason to reject sets *A* and *D*. The experimental spectra also show a common feature at 423 cm^{-1} (52 meV). This is largely masked by the main "phosphorus" peak in the boron-phosphorus spectrum, but shows up clearly in the boron-arsenic spectrum. Only set *C* gives a clear feature in this region (which is again associated with a density of modes peak) but this is much weaker than the observed feature.

We therefore favor sets *B* and *C* but cannot choose between them. It will be noted that the most striking difference between them is the sign of η_0, which has the same sign as the static charge in set *B* but the opposite sign in set *C*. Either sign is possible since there is no simple relation between apparent and static charges, as is evidenced by the large apparent charge on the neutral carbon impurity in silicon.[34]

VI. CONCLUSIONS

We have confirmed the suggestion by Angress *et al.*[11] that the presence of the sharp resonance (quasilocal mode) at 227 cm^{-1} in the absorption due to substitutional B in Si implies that the bond-bending force constant at the impurity is stronger than in the host. This is in disagreement with the claim by Cardona *et al.*[5] that this feature may be understood in terms of the mass defect alone. We find that although there is a peak in this region of the calculated absorption spectrum when force-constant changes are neglected (and only the impurity carries an apparent charge, as assumed by Cardona *et al.*) it is lower in frequency (219 cm^{-1}) and broader than the experimental peak. Cardona *et al.* base their claim on a belief that the falloff in the density of TA modes is sufficiently sudden to be approximated by a step function. This would lead, in the usual way, to a logarithmic singularity in the real part of the perfect-lattice self-Green's-function and so to a "gap" mode for any impurity with lighter mass than the host. This gap mode would then be broadened by interaction with the weak LA background. (See also Shen *et al.*[35]) However, we have shown (see Appendix A) that with a realistic density of modes this does not happen. Instead it is the strengthening of the bond-bending force constant which is responsible for pushing the absorption peak up to a frequency where the density of modes is low and so the peak is sharp.

There are some interesting parallels between the 227-cm^{-1} resonance and the absorption peak around 330 cm^{-1}. In the calculated absorption the frequency of the latter is again significantly higher than the frequency of the associated density of modes peak; it may therefore also be described as a resonance. For our model there is a peak in the density of modes at 327 cm^{-1}. For ^{11}B and no change in force constants (or with $\delta\beta=0$ and $\delta\alpha=-4.13$ N/m, see Sec. V) the peak in the absorption, calculated with an apparent charge on the impurity only, lies at 333 cm^{-1}. With our final values of $\delta\alpha$ and $\delta\beta$ [Eq. (3.10)] the peak moves up to 335 cm^{-1}. Although the increase $\delta\beta$ in the bond-bending force constant leads in this case to a rather small frequency shift, it does lead to a reduction in the left-hand side of the resonance criterion (A1) very similar to that for the lower-frequency peak. (See Fig. 5.) The resonance criterion is not quite satisfied, but a further increase in $\delta\beta$ (and corresponding decrease in $\delta\alpha$ to keep the local mode at its observed frequency) sufficient to bring the left-hand side (lhf) of (A1) below zero raises the frequencies of both the 335-cm^{-1} peak and the 227-cm^{-1} peak by only ~ 1 cm^{-1}. The higher peak remains relatively wide because the density of modes is relatively high. The difference between the absorption and the density of modes appears just as a shift in peak position because the peak in the density of modes is itself rather narrow.

We turn now to the strengths of the various features in the absorption spectrum. We have illustrated for the first time the effects on these of the apparent charges on neighbors of the impurity, making detailed calculations which include first and second neighbors. By making use of the sum rule (4.4) and assigning to the second neighbors apparent charges given by the asymptotic expressions (4.1) the number of unknown apparent charges was reduced to two. These were fitted to the strength of the local mode and the 227-cm^{-1} resonance. From the resulting four sets of apparent charges we eliminated two because they made the peak around 330 cm^{-1} much stronger than is observed, but we are unable to choose between the remaining two. These differ mainly in the signs of the apparent charges of the impurity itself and its nearest neighbors; there is as yet no reliable theoretical prediction for this sign.

We have also shown that the absorption due to

the electric field induced apparent charges of more distant neighbors is concentrated near the top of the band and is responsible for the sharp step in absorption observed there in crystals compensated with a group-V impurity. The contribution of these distant neighbor apparent charges to the integrated absorption is comparable in magnitude with the *in-band* contribution of the apparent charges of the impurity and its first and second neighbors.

There is a need for further calculations to determine the detailed effects of the apparent charges of third and further neighbors on the spectral form of the absorption. It will, of course, be essential to employ a better model than we have used for the lattice dynamics of the host crystal since in our simple model the dispersion of the optical branches is poorly represented. Because of the large number of distant neighbors whose apparent charges make an important contribution to the absorption it will almost certainly be necessary to extend conventional techniques to allow for a continuum approximation of the Green's functions connecting well-separated atoms.

ACKNOWLEDGMENTS

We are grateful to Professor R. C. Newman for drawing our attention to the recent revival of interest in the 227-cm^{-1} quasilocal mode in boron-doped silicon stimulated by the observation of similar modes in boron-doped GaAs and GaP. His encouragement and comments throughout this work have been of great value. We are indebted to Dr. A. C. R. Thornton and other staff of Reading University Computer Centre for their assistance in using local facilities and those of the University of Manchester Regional Computer Centre. The results of this appendix were obtained originally by one of us (R.S.L.) and Professor B. Szigeti and were communicated privately to Professor R. C. Newman, who refers to them[1], but they were otherwise not published until now.

APPENDIX A: APPROXIMATE FREQUENCY AND EIGENVECTOR FOR THE QUASILOCAL MODE

Maradudin[26] gives as a criterion for the occurrence of an in-band resonance at frequency ω the vanishing of the real part of an eigenvalue of the matrix (in our notation and in the defect subspace for Γ_5 symmetry)

$$\underline{\underline{I}}+\underline{\underline{G}}(\Gamma_5{:}\omega)\underline{\underline{D}}(\Gamma_5{:}\omega)\ .$$

Talwar and Agrawal[17,28] use for this purpose the vanishing of the real part of the determinant of this matrix. We have used in Sec. III the vanishing of the determinant of the real part of the matrix, i.e.,

$$|\underline{\underline{I}}+\mathrm{Re}\underline{\underline{G}}(\Gamma_5{:}\omega)\underline{\underline{D}}(\Gamma_5{:}\omega)|=0\ . \tag{A1}$$

The smaller the imaginary parts of the perfect-lattice Green's functions, the closer are the three criteria. In the present problem we find no significant difference between them, i.e., no more than 0.1 cm^{-1} in the position of the quasilocal mode. In Fig. 5 we show the lhs of Eq. (A1), as a function of ω in the band, for ^{11}B and our final values of $\delta\alpha$ and $\delta\beta$ [Eq. (3.10)], and also for the pure mass defect (when all three criteria are the same because only one element of $\underline{\underline{D}}$ is nonzero). We note that although in the latter case there is a minimum at 219 cm^{-1}, which is the position of a maximum in the absorption (see Sec. V), it comes nowhere near zero. The same is true for $\delta\beta=0$ and $\delta\alpha=-4.13\ \mathrm{N\,m^{-1}}$ (see Sec. V).

It is of some interest that for the final values of $\delta\alpha$ and $\delta\beta$ the curve falls nearly to zero at 332 cm^{-1} which is close to the frequency of a feature in the calculated absorption (see Figs. 3 and 4) and significantly higher than the frequency of the associated density of modes peak. This is discussed further in Sec. VI.

The eigenvector of a true local mode is obtained from the behavior of the modified Green's functions in the neighborhood of the frequency ω_0 of the mode, since these have a pole there with residue [coefficient of $1/(\omega-\omega_0)$]

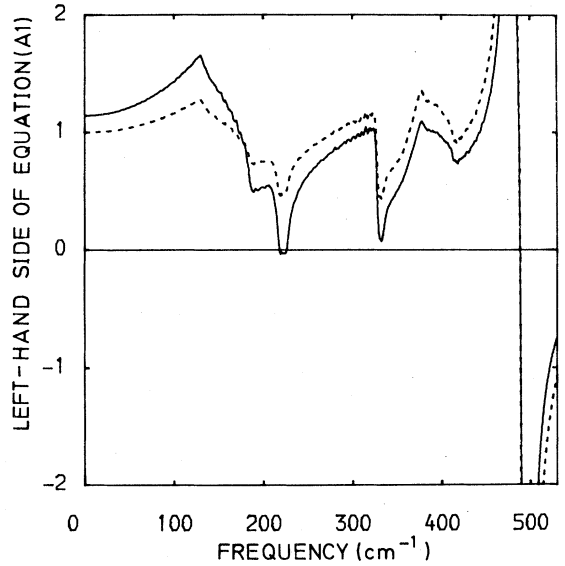

FIG. 5. Left-hand side of resonance condition (A1). Solid curve is for $\delta\alpha=-6.34$ N/m and $\delta\beta=7.55$ N/m; dotted curve is for $\delta\alpha=\delta\beta=0$.

$$-u_{n\alpha}u_{n'\beta}/(2\omega_0)$$

for $G'_{n\alpha,n'\beta}(\omega)$. $u_{n\alpha}$ is the α component of the displacement in the mode of the nth atom, normalized in the usual way so that

$$\sum_{n\alpha} m_n u_{n\alpha}^2 = 1 .$$

In our calculations we have of course used the Γ_5 symmetry-adapted Green's functions and displacements [see Eqs. (3.4) and (3.6)]. We have obtained an "eigenvector" for the quasilocal mode in the same way by using the *real* parts of the perfect-lattice Green's functions when determining the modified Green's functions [Eq. (3.8)]. The latter have a pole at the frequency given by (A1). Although strictly the quasilocal mode does not have an eigenvector, the eigenvector obtained in this way is obviously a useful construct provided the resonance is sufficiently sharp. It is this eigenvector which has been used to calculate the quasilocal mode dipole moments (Table V).

APPENDIX B: EXPERIMENTAL VALUES FOR PHOTOELASTIC AND RAMAN CONSTANTS

The most recent values of the photoelastic constants of silicon below the absorption edge are those of Biegelson,[37,38] who measured p_{11} and p_{12} at wavelengths of 3.39 and 1.15 μm, and p_{44} at 3.39 μm, by diffraction from acoustic waves. Extrapolation to infinite wavelength gave

$$p_{11} = -0.093, \quad p_{12} = +0.019 .$$

These values are considerably different from the older values used by Leigh and Szigeti,[21] but are in excellent agreement with a very recent measurement at helium temperature and 3 kHz by Tan and Castner[39] of

$$\frac{1}{\epsilon_0}\frac{\partial \epsilon_{zz}}{\partial \sigma_{110}} = -\frac{\epsilon_0}{3}\left[\frac{p_{11}+2p_{12}}{C_{11}+2C_{12}} - \frac{p_{11}-p_{12}}{C_{11}-C_{12}}\right], \tag{B1}$$

where σ_{110} is a tensile stress in the [110] direction and C_{11}, etc., are the usual elastic constants. The measured value is -3.37×10^{-7} cm^2/kg while the value of the right-hand side (using the elastic constants of McSkimin and Andreatch[40]) is -3.54×10^{-13} cm^2/dyn, i.e., -3.48×10^{-7} cm^2/kg. Higginbotham *et al.*[41] have made the most recent measurements of the static stress-induced birefringence for [001] and [111] stress between 2.5 μm and the absorption edge. Extrapolation to infinite wavelength gave values which, when combined with the elastic constants, yield

TABLE VII. Values of $|\beta_R r_0|$ obtained from various combinations of experiment and theory. See text for an explanation of methods I and II and the significance of the references for method I. The infinite wavelength values quoted rely on the dispersion of the Raman tensor calculated by Swanson and Maradudin (Ref. 48, column headed SM) and Wendel (Ref. 49, column headed W).

Method	Refs.	SM	W
I	a,b,c	0.10	0.14
	d,b,c	0.07	0.10
II	e	0.18 (±0.06)	0.23 (±0.08)

[a]Reference 43.
[b]Reference 50.
[c]Reference 51.
[d]Reference 42.
[e]Reference 47.

$$p_{11}-p_{12} = -0.127, \quad p_{44} = -0.050 .$$

This extrapolated value of p_{44} agrees well with Biegelson's value at 3.39 μm (-0.051), and we shall use it. The value of $p_{11}-p_{12}$ is in only fair agreement with Biegelson, and if used, for example, in conjunction with Biegelson's p_{11} to determine p_{12} ($+0.034$), leads to -4.43×10^{-7} cm^2/kg for the right-hand side of (B1). We shall therefore use Biegelson's values of p_{11} and p_{12}.

Reported determinations of the magnitude of the Raman tensor for silicon have employed two methods, referred to as I and II in Table VII. In method I (Refs. 42 and 43) the ratio of the Raman-scattering intensities of silicon and diamond is measured. The magnitude of the Raman tensor for diamond has been determined in various ways,[31,44–46] the most recent of which relies on the relative intensity of Raman and Brillouin scattering from the same crystal.[45,46] The intensity of Brillouin scattering depends in turn on the photoelastic constants which have to be measured independently. In method II the relative intensity of Raman and Brillouin scattering is measured in silicon itself.[43,47] Both methods have been carried out at several wavelengths, all well above the indirect absorption edge of silicon. To obtain a value at infinite wavelength some assumption must be made about the dispersion. Swanson and Maradudin[48] and Wendel[49] have calculated the Raman tensor of silicon as a function of frequency using pseudopotential energy bands and matrix elements. They disagree on both dispersion and absolute magnitude. Their infinite wavelength results correspond to $|\beta_R r_0| = 0.04$ and 0.13, respectively, although because of the slightly too small theoretical band gap Wendel[49] estimates

that his magnitude should perhaps be reduced by up to 20%.

The infinite wavelength values in Table VII have been obtained using the dispersion (but not the magnitude) calculated in Refs. 48 and 49. The values in the first line of the table use the following.

(i) The ratio of Raman-scattering intensities of silicon and diamond measured at 1.92 eV and deduced from Fig. 1 of Ref. 43 knowing the value used there for the Raman tensor of diamond.

(ii) The value for the Raman tensor of diamond at 1.92 eV obtained from the value at 2.41 eV recommended by Cardona[50] with a small correction for dispersion following the simplified E_0' edge calculation of Calleja *et al.*[51] (see also Ref. 50).

The values in the second line come from using, instead of (i) above, the early determination by Russell[42] of the silicon-diamond ratio at 1.96 eV. Taking into account the results of methods I and II Cardona[50] recommends a value for silicon at 1.9 eV which is equivalent to $|\beta_R r_0| = 0.12 \pm 0.04$ using the dispersion of Ref. 48 and 0.16 ± 0.05 using that of Ref. 49.

The sign of the Raman tensor in silicon has been determined by Cardona *et al.*[52] from an analysis of the observed antiresonance in the Raman spectrum of heavily doped *p*-type silicon caused by interference between phonon scattering and inter-valence-band electronic scattering. If an *A* sublattice atom has a *B* sublattice neighbor at $(a/4)(1,1,1)$, β_R is found to be negative. (This agrees with the sign found in both theoretical calculations.[48,49])

In the calculations of this paper we have used $\beta_R r_0 = -0.1$, which is supported by the values in Table VII for method I but not by the surprisingly high values for method II.

APPENDIX C: ABSORPTION DUE TO LONG-RANGE ELECTRIC FIELD

Apparent charges induced on distant neighbors of a charged impurity (or of any charged defect) via the Raman tensor of the host lattice and the electric field of the impurity [see Eq. (4.1)] activate the long-wave optical modes of the host in the same way as does an external electric field. We now consider the spectral dependence of this absorption. In the long-wavelength limit the optical modes of the host may be described in terms of spatially slowly varying sublattice displacements, equal and opposite on the two sublattices, and we are free to choose this spatial dependence to be $\sin\vec{k}\cdot\vec{r}$ or $\cos\vec{k}\cdot\vec{r}$ with respect to an arbitrary origin of $\vec{r}$. With the position of the impurity chosen as origin it follows from the proportionality of the apparent charges to the Coulomb field of the impurity that only the $\sin\vec{k}\cdot\vec{r}$ modes are activated. Moreover, since the impurity and its nearest neighbors are essentially stationary, these modes are unaffected by the presence of the impurity.

Let $\hat{e}^j(\hat{k})$ $(j=1,2,3)$ denote orthogonal unit vectors in the directions of sublattice displacement for the optical modes with wave vector $\vec{k}$; as indicated these depend, in the small-k limit, on the *direction* of $\vec{k}$ but not its magnitude. If $Q^j(\vec{k})$ is the normal coordinate of the jth mode at $\vec{k}$, the displacement at $\vec{r}$ of one sublattice in this mode is equal to

$$\frac{1}{2}\left[\frac{a^3}{m_{\mathrm{Si}}V}\right]^{1/2} Q^j(\vec{k})\hat{e}^j(\hat{k})\sin\vec{k}\cdot\vec{r}\,,$$

where V is the volume of the crystal. The Raman contribution to the z component of the mode dipole moment from one atom *pair* at $\vec{r}$ is then

$$M_z^j(\vec{k}) = \frac{1}{16\pi}\left[\frac{a^3}{m_{\mathrm{Si}}V}\right]^{1/2} Q^j(\vec{k}) Ze\epsilon_0\beta_R \left[\frac{a}{r}\right]^3 [y e_x^j(\hat{k}) + x e_y^j(\hat{k})]\sin\vec{k}\cdot\vec{r}\,. \tag{C1}$$

We sum this over all atom pairs at a distance from the impurity greater than r_c, and replace the sum by an integral. Since

$$\int_{(r>r_c)} dV \frac{x}{r^3}\sin\vec{k}\cdot\vec{r} = -\frac{\partial}{\partial k_x}\int_{(r>r_c)} dV \frac{\cos\vec{k}\cdot\vec{r}}{r^3} = 4\pi\frac{k_x}{k^3}\frac{\sin kr_c}{r_c}$$

(and similarly for the y component) we find

$$\left[\frac{\partial M_z^j(\vec{k})}{\partial Q^j(\vec{k})}\right]^2 = \frac{16}{3}\frac{a}{m_{\mathrm{Si}}V}(e\epsilon_0\beta_R r_0)^2\frac{\sin^2 kr_c}{k^6 r_c^2}[k_y e_x^j(\hat{k}) + k_x e_y^j(\hat{k})]^2\,. \tag{C2}$$

The dispersion of the long-wave optical modes is given by

$$\omega^j(\vec{k}) = \omega_R[1 - \tfrac{1}{2}\lambda^j(\hat{k})(ak/2\pi)^2]\,, \tag{C3}$$

where ω_R denotes the Raman frequency and $\lambda^j(\hat{k})$ is a dimensionless parameter that depends on j and the

direction of $\vec{k}$. Denoting by $k^j(\hat{k},\omega)$ the magnitude of $\vec{k}$ corresponding to a given frequency ω for the jth branch in direction $\hat{k}$ we find finally for the cross section near ω_R

$$\sigma(\omega)=\frac{2\pi^2}{\rho c}\frac{1}{2}\sum_{\vec{k}}\sum_{j}\left[\frac{\partial M_z^j(\vec{k})}{\partial Q^j(\vec{k})}\right]^2\delta(\omega-\omega^j(\vec{k}))$$

$$=\frac{4}{3\sqrt{2}}\frac{(e\epsilon_0\beta_R r_0)^2}{\rho c m_{\mathrm{Si}}}\frac{1}{{\omega_R}^{1/2}}\frac{1}{(\omega_R-\omega)^{1/2}}\sum_j\int d\hat{k}[\lambda^j(\hat{k})]^{-1/2}$$

$$\times\left[\frac{\sin(k^j(\hat{k},\omega)r_c)}{k^j(\hat{k},\omega)r_c}\right]^2[\hat{k}_y e_x^j(\hat{k})+\hat{k}_x e_y^j(\hat{k})]^2\,, \tag{C4}$$

where the summation over $\vec{k}$ and corresponding integration over $\hat{k}$ are over all directions (rather than half). This integral tends to a constant as $\omega\to\omega_R$. The infinity in $\sigma(\omega)$ at $\omega=\omega_R$ will of course be removed by anharmonic broadening, leading to a peak slightly below ω_R and a sharp falloff on the high-frequency side as is observed.

It is straightforward to show that for this contribution to the cross section

$$\int^{\omega_R}\sigma(\omega)d\omega=\frac{8\pi}{9}\frac{(e\epsilon_0\beta_R r_0)^2}{\rho c m_{\mathrm{Si}}}\frac{a}{r_c}\,. \tag{C5}$$

First the integration over ω is performed by converting it to an integration over k, which is then extended to infinity as is appropriate in a macroscopic approximation. The integration over $\hat{k}$ is then possible using the orthonormality of the $\hat{e}^j(\hat{k})$. About 80% of the total is contributed by k values up to a third of the way to the Brillouin zone boundary. The various approximations we have made are not unreasonable for these values of k. The result for $\int\sigma(\omega)d\omega$ agrees, as it must, with the result of Eq. (4.3) if we replace the sum by an integral from r_c to infinity and include only the Raman contributions to the apparent charges. The numerical value of the integral, if r_c is equal to the radius of a sphere whose volume is that of 17 atoms (impurity plus two shells of neighbors), is 12×10^{-19} cm (frequency in cm^{-1}). That this value is exactly equal (to the quoted accuracy, and in fact to 1%) to that taken in Sec. V for the integrated cross section from third neighbors and beyond is fortuitous. The calculation of Sec. V included photoelastic contributions to the apparent charges and, for the first few shells, the summation in Eq. (4.3) was not replaced by an integral. In addition, it would be wrong to conclude that photoelastic contributions to apparent charges beyond second neighbors will have no effect on the spectral distribution of the absorption.

The above results are for an isolated impurity. The result for the contribution to the integrated absorption also applies to a *random* distribution of charged impurities or defects at low concentrations, because then the mean of the square of a component of the electric field is (per impurity) the same as for an isolated impurity. The integrated absorption would however be reduced if there were positive (negative) correlation between the positions of impurities of opposite (the same) charge such as may be introduced into the crystal during preparation while still molten. An extreme example of this occurs in the Li-compensated crystals in which the Li^+ and B^- are nearly all in close pairs and do not give rise to long-range monopole fields. Unfortunately, however, the available measurements[2–5,53] provide no evidence either for or against the presence of a sharp drop in absorption at the Raman frequency. Such a feature would be masked by the strong ^{7}Li line which overlaps the Raman frequency and is present to some extent even in ^{6}Li enriched samples. Boron-phosphorus close pairs would similarly have no long-range monopole field and there may be[1] up to 20% of these in the samples of Angress *et al.*[6] On the other hand, doubly charged boron-boron close pairs would enhance the absorption step.

[1]R. C. Newman, *Infrared Studies of Crystal Defects* (Taylor and Francis, London, 1973).

[2]M. Balkanski, in *Proceedings of the 7th International Conference on Physics of Semiconductors, Paris, 1964,* edited by M. Hulin (Academic, London, 1964), pp. 1021–1036; M. Balkanski and W. Nazarewicz, J. Phys. Chem. Solids 27, 671 (1966).

[3]W. G. Spitzer and M. Waldner, Phys. Rev. Lett. 14, 223 (1965); J. Appl. Phys. 36, 2450 (1965).

[4]R. M. Chrenko, R. S. McDonald, and E. M. Pell, Phys. Rev. A 138, 1775 (1965).

[5]M. Cardona, S. C. Chen, and S. P. Varma, Phys. Rev. B 23, 5329 (1981).

[6]J. F. Angress, A. R. Goodwin, and S. D. Smith, Proc. R.

Soc. London, Ser. A 287, 64 (1965).
[7]J. F. Angress, A. R. Goodwin, and S. D. Smith, Proc. R. Soc. London Ser. A 308, 111 (1968).
[8]G. Dolling, in *Inelastic Scattering of Neutrons in Solids and Liquids* (IAEA, Vienna, 1963), Vol. II, pp. 37–48.
[9]G. Nilsson and G. Nelin, Phys. Rev. B 6, 3777 (1972).
[10]P. N. Keating, Phys. Rev. 145, 637 (1966).
[11]J. F. Angress, G. A. Gledhill, and R. C. Newman, J. Phys. Chem. Solids 41, 341 (1980).
[12]G. A. Gledhill, S. S. Kudhail, R. C. Newman, and G. Z. Zhang, Int. J. Infra. Millimeter Waves 2, 849 (1981).
[13]P. G. Dawber and R. J. Elliott, Proc. Phys. Soc. London 81, 453 (1963).
[14]G. Dolling and R. A. Cowley, Proc. Phys. Soc. London 88, 463 (1966).
[15]W. Weber, Phys. Rev. B 15, 4789 (1977).
[16]R. S. Leigh and B. Szigeti, Proc. R. Soc. London Ser. A 301, 211 (1967).
[17]D. N. Talwar and B. K. Agrawal, J. Phys. Chem. Solids 39, 207 (1978).
[18]Y. Ikuta, A. Manabe, A. Mitsuishi, H. Komiya, and S. Ibuki, Opt. Comm. 5, 285 (1972).
[19]R. S. Leigh and B. Szigeti, Phys. Rev. Lett. 19, 566 (1967).
[20]R. S. Leigh and B. Szigeti, in *Proceedings of the Irvine Conference on Localized Excitations in Solids,* edited by R. F. Wallis (Plenum, New York, 1968), pp. 159–166.
[21]R. S. Leigh and B. Szigeti, J. Phys. C 3, 782 (1970).
[22]R. S. Leigh and M. J. L. Sangster, J. Phys. C 15, L317 (1982).
[23]R. M. Martin, Phys. Rev. B 1, 4005 (1970).
[24]G. A. Baraff, E. O. Kane, and M. Schlüter, Phys. Rev. B 21, 5662 (1980).
[25]H. W. Icenogle, B. C. Platt, and W. L. Wolfe, Appl. Opt. 15, 2348 (1976).
[26]A. A. Maradudin, in *Solid State Physics,* edited by F. Seitz and D. Turnbull (Academic, London, 1966), Vol. 19, pp. 1–134; See also A. A. Maradudin, E. W. Montroll, G. H. Weiss, and I. P. Ipatova, *Solid State Physics,* edited by H. Ehrenreich, F. Seitz, and D. Turnbull (Academic, London, 1971) Suppl. 3, 2nd ed.; The Green functions in our expressions are defined by $\underline{G}=[\underline{\Phi}-(\omega^2+i0)\underline{m}]^{-1}$, where $\underline{\Phi}$ is the force-constant matrix and $\underline{m}$ the diagonal matrix of masses.
[27]F. Herman, J. Phys. Chem. Solids 8, 405 (1959).
[28]D. N. Talwar and B. K. Agrawal, Phys. Rev. B 9, 4362 (1974).
[29]G. Herzberg, *Molecular Spectra and Molecular Structure II: Infrared and Raman Spectra of Polyatomic Molecules* (Van Nostrand, Princeton, 1945).
[30]J. F. Angress, C. Cooke, and A. J. Maiden, J. Phys. C 1, 1769 (1968).
[31]E. Anastassakis, S. Iwasa, and E. Burstein, Phys. Rev. Lett. 17, 1051 (1966). E. Anastassakis and E. Burstein, Phys. Rev. B 2, 1952 (1970).
[32]L. Kleinman, in *Proceedings of the International Conference on the Physics of Semiconductors, Exeter, 1962,* edited by A. C. Stickland (Institute of Physics and the Physical Society, London, 1962), pp. 552–558. We have used $\zeta=0.62$, the measured value of Segmüller and Neyer, Phys. Kondens. Mater. 4, 63 (1965). ζ has been remeasured very recently by H. d'Amour, W. Denner, H. Schulz, and M. Cardona, J. Appl. Crystallogr. 15, 148 (1982), who find $\zeta=0.74$, and by C. S. G. Cousins, L. Gerward, J. S. Olsen, B. Selsmark, and B. J. Sheldon, *ibid.* 15, 154 (1982), who find $\zeta=0.72$.
[33]A. R. Goodwin, Ph.D. thesis, University of Reading, United Kingdom, 1966 (unpublished).
[34]R. C. Newman and J. B. Willis, J. Phys. Chem. Solids 26, 373 (1965).
[35]S. C. Shen, C. J. Fang, and M. Cardona, Phys. Status Solidi B 101, 451 (1980); the early mass defect calculation of Bellomonte and Pryce (Ref. 36) for B in Si, referred to by these authors, also uses a density of modes with an unrealistically sharp falloff at the top of the TA region.
[36]L. Bellomonte and M. H. L. Pryce, in *Proceedings of the Irvine Conference on Localized Excitations in Solids,* edited by R. F. Wallis (Plenum, New York, 1968), pp. 203–209.
[37]D. K. Biegelson, Phys. Rev. Lett. 32, 1196 (1974).
[38]D. K. Biegelson, Phys. Rev. B 12, 2427 (1975).
[39]H. S. Tan and T. E. Castner, Phys. Rev. B 23, 3983 (1981).
[40]H. J. McSkimin and P. Andreatch, J. Appl. Phys. 35, 2161 (1964).
[41]C. W. Higginbotham, M. Cardona, and F. H. Pollak, Phys. Rev. 184, 821 (1969).
[42]J. P. Russell, Appl. Phys. Lett. 6, 223 (1965).
[43]M. Grimsditch and M. Cardona, in *Proceedings of the 14th International Conference on Physics of Semiconductors, Edinburgh, 1978,* edited by B. L. H. Wilson (Institute of Physics, London, 1979), pp. 639–642.
[44]A. K. McQuillan, W. R. L. Clements, and B. P. Stoicheff, Phys. Rev. A 1, 628 (1970).
[45]M. Grimsditch and A. K. Ramdas, Phys. Rev. B 11, 3139 (1974).
[46]M. Grimsditch, M. Cardona, J. M. Calleja, and F. Meseguer, J. Raman Spectros. 10, 77 (1981).
[47]M. Grimsditch and M. Cardona, Phys. Status Solidi B 102, 155 (1980).
[48]L. Swanson and A. A. Maradudin, Solid State Commun. 8, 859 (1970).
[49]H. Wendel, Solid State Commun. 31, 423 (1979).
[50]M. Cardona, in *Light Scattering in Solids II,* edited by M. Cardona and G. Guntherodt (Springer, New York, 1982), p. 92.
[51]J. M. Calleja, J. Kuhl, and M. Cardona, Phys. Rev. B 17, 876 (1978).
[52]M. Cardona, F. Cerdeira, and T. A. Fjeldy, Phys. Rev. B 10, 3433 (1974).
[53]R. C. Newman and D. H. J. Totterdell, J. Phys. C 7, 3418 (1974).